MODELING THE DESTRUCTION OF ICE JAMS

V. I. Odinokov and A. N. Prokudin

UDC 539.3

Elastic small-deformation theory, the equations of hydrodynamics, and a well-tested numerical method are used to solve the axisymmetric problem of determining the stress–strain state in a complex multicomponent system with an ice plate of finite thickness subjected to dynamic loading.
     Key words: *destruction of ice cover, stress, deformation, dynamic effect.*

Introduction. As is known, in the ice breakup period, especially in Siberia, ice jams cause a water level rise and flooding. At present, the destruction of ice jams is usually performed by bombing, which produces a dynamic explosive load on ice, leading to its breakup. This method has a negative effect on water fauna and requires large power consumptions.

In the present paper, a mathematical model is constructed for an ice breaking method in which a device consisting of two cylinders enclosed one into another is placed under ice or an ice jam (Fig. 1). The bottom of the upper cylinder with the greater inner diameter faces the lower surface of ice. In the lower cylinder, whose bottom faces the bottom of the water reservoir, there are channels housing a flexible system consisting of a gas hose and a power line. Buoyancy and maneuverability of the structure is provided by engines and a chamber which can be filled with water or air.

The process is implemented as follows.

The device equipped with video cameras and locomotive means operated from a mobile station located on the coast using the flexible system is placed under an ice jam. After the placement of the device under the ice jam, the gap between the cylinders is filled with a definite volume of an air–gas mixture (natural gas) through the flexible system from the station certain volume acts. After that, a spark is applied to the plugs. The air–gas mixture is exploded, causing the lower cylinder to rush downward and the upper cylinder upward and destroying a local region of the ice jam. The movement of the lower cylinder downward is prevented by water, and, possibly, the bottom of the reservoir. The surfaces of the cylinders sliding relative to each other are furnished with a system for restricting their vertical movement to prevent one cylinder from falling out of the other. After explosion, the gas escapes through numerous holes on the walls of the cylinder, and the device returns to the initial position and moves under ice to another region under the jam.

Formulation of the Problem. The computation diagram of the deformation process is presented in Fig. 2. Region I is ice acted upon by the pressures p_1 and p_2 which vary in both size and the coordinate x_2: $p_1 \geqslant p_{\text{atm}}$ and $p_2 \geqslant p_{\text{atm}}$ (p_{atm} is atmospheric pressure). One cannot use only one function of external loading, for example, $p_1 = p_1(x_2)$ because, at $x_2 = R_3$, the function $p_1(x_2)$ can undergo a discontinuity. It is more convenient to introduce one more function of the external pressure $p_2\big|_{x_2 > R_3} = p_2(x_2)$. Regions II and III are the upper and lower cylinders, region IV is water, and region V is the gas occupying the space between the two cylinders. The peripheral region $x_2 \geqslant R_5$ is at a significant distance from regions II and III: $R_5 \gg R_4$. Thus, we have a five-component system. The media corresponding to regions I–IV are considered isotropic and incompressible, and the deformations in regions I–III are small. In region V, the initial pressure p_3 depends on the composition and burning velocity of the gas and the thickness of the gas cushion H_4.
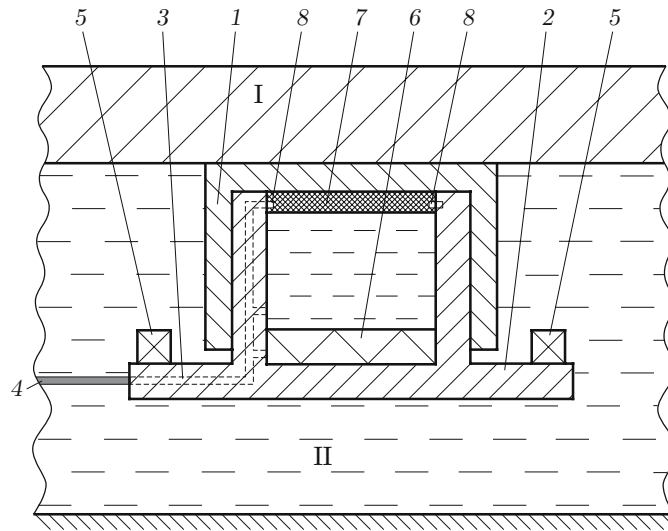
Fig. 1. Diagram of the device for breaking ice: ice (I) and water (II); 1) upper cylinder; 2) lower cylinder; 3) channels; 4) flexible system including a gas hose and an electricity cable; 5) engines; 6) chamber; 7) air–gas mixture; 8) plugs.
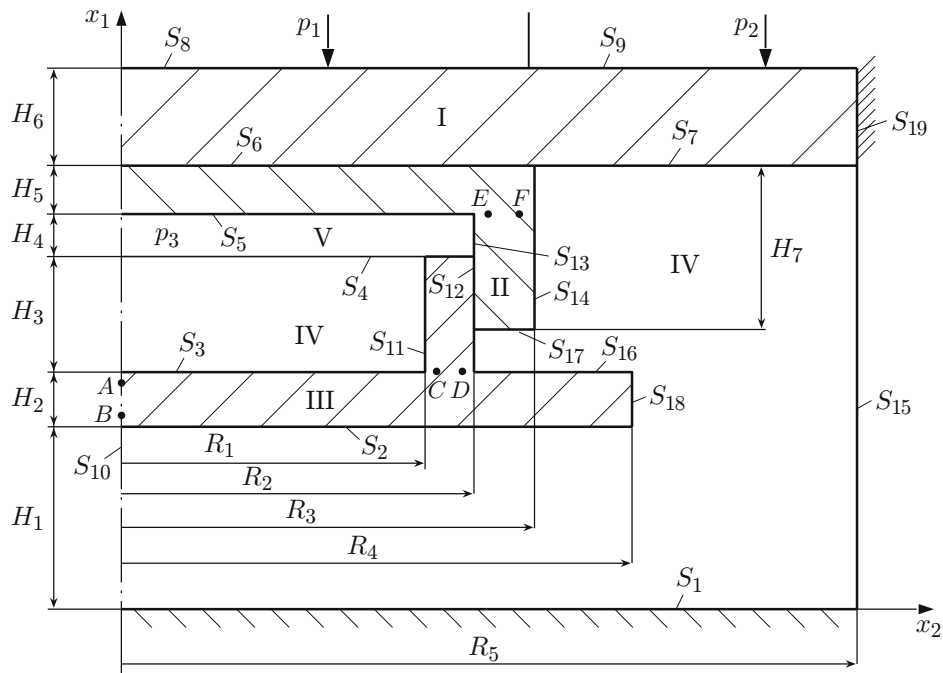

Fig. 2. Computation diagram of deformation: ice (I), upper cylinder (II), lower cylinder (III), water (IV), and gas (V); A, B, C, D, E, and F are the points of extreme stresses σ_{11} and σ_{22}.

Using the formulated assumptions, we write the following system of differential equations in Cartesian coordinates for the corresponding regions.

The elastic incompressible medium (regions I–III) is described by the following equations of elastic small-deformation theory:

— the equations of motion

$$\sigma_{ij,j} + F_i^t = I_i^t, \qquad I_i^t = \rho_t \frac{dv_i}{d\tau},$$

$$\frac{dv_i}{d\tau} = \dot{v}_i + v_k \frac{\partial v_i}{\partial x_k}, \qquad i,j,k = 1,2,3; \tag{1}$$

— the equations of state (Hooke's law)

$$\sigma_{ij} - \sigma\delta_{ij} = 2G_t\varepsilon_{ij}, \qquad \delta_{ij} = \begin{cases} 1, & i = j, \\ 0, & i \neq j, \end{cases}$$

$$i = 1,2,3, \qquad \varepsilon_{ij} = 0.5(u_{i,j} + u_{j,i}); \tag{2}$$

— the incompressibility equation

$$v_{i,i} = 0. \tag{3}$$

In Eqs. (1)–(3), the summation is performed over the repeated indices, $[\sigma_{ij}]$ is the stress tensor, $[\varepsilon_{ij}]$ is the strain tensor, $\sigma = \sigma_{ii}/3$ is the hydrostatic stress, v_i is the projection of the displacement rate onto the coordinate axes x_i ($i = 1,2,3$), ρ_t is the density of the material, F_i^t is the projection of the specific bulk force onto the coordinate axes x_i ($i = 1,2,3$) in the corresponding region $t = \text{I}, \text{II}, \text{III}$, $\dot{v}_i = \partial v_i/\partial \tau$ (dot above the symbol denotes the time derivative), τ is a monotonic deformation parameter, G_t is the shear modulus in the region of t, and I_i^t is the projection of the inertial force normalized to unit volume onto the coordinate axes x_i; the subscript t takes values I, II, and III.

Small strains obey the relations

$$\frac{d\varepsilon_{uj}}{d\tau} = \xi_{ij} \quad \Rightarrow \quad \varepsilon_{ij} = \int_\tau \xi_{ij}\, d\tau, \qquad \xi_{ij} = 0.5(v_{i,j} + v_{j,i}),$$

where ξ_{ij} are the components of the strain rate tensor $[\xi_{ij}]$ and $v_{i,j} = \partial v_i/\partial x_j$.

For deformation ($\tau = \sum \tau_m$) which is discrete in time τ, the strain is expressed in difference form

$$(\varepsilon_{ij})_m \simeq \sum_m (\xi_{ij})_m \,\Delta\tau_m = (\varepsilon_{ij})_{m-1} + (\xi_{ij})_m \,\Delta\tau_m,$$

where $\Delta\tau_m$ are the steps in the parameter τ, $(\xi_{ij})_m$ are the strain tensor components rate in the step $\Delta\tau_m$, $(\varepsilon_{ij})_m$ are the strain tensor components in the time step m, and $(\varepsilon_{ij})_{m-1}$ are the strain tensor components in the time step $m - 1$.

For the incompressible liquid: $\rho = \text{const}$ (region IV) the following system of hydrodynamic equations holds:
— the momentum conservation law

$$F_i^t - \frac{\partial p}{\partial x_i} + \mu\nabla^2 v_i = I_i^t, \qquad I_i^t = \rho_t\frac{dv_i}{d\tau}, \qquad i = 1,2,3; \tag{4}$$

— the incompressibility equation

$$v_{i,i} = 0. \tag{5}$$

In (4) and (5), $p = -\sigma$ is the pressure at this point, μ [g$\cdot$ sec/cm^2] is the liquid viscosity, and ∇^2 is the Laplace operator:

$$\nabla^2 v_i = \frac{\partial^2 v_i}{\partial x_1^2} + \frac{\partial^2 v_i}{\partial x_2^2} + \frac{\partial^2 v_i}{\partial x_3^2}.$$

For the gas (region V), we specify the pressure p_3 that arises from the combustion of the air–gas mixture in the closed volume and depends on the composition and burning velocity of the gas. Gas combustion is a chemical reaction involving release of combustion products at a high temperature. The combustion temperature can exceed 2000°C [1], resulting in an increase in the gas pressure in the closed volume. The pressure p_3 and burning velocity v_b are specified using experimental data [1]. The burning time is determined by the thickness of the gas cushion

95

H_4: $\tau_b = H_4/v_g$. The reaction time is short (about 0.1 sec); therefore, it can be assumed that, after the burnup of the air–gas mixture, the pressure depends only on the volume change, i.e., $p_3 V = \text{const}$.

Because of the axial symmetry of the problem ($v_3 = 0$ and $\sigma_{31} = \sigma_{32} = 0$), the boundary conditions (for the notation see Fig. 2) become

$$\sigma_{11}\Big|_{S_i} = -p_3 \quad (i = 4, 5), \qquad \sigma_{11}\Big|_{S_8} = -p_1, \qquad \sigma_{11}\Big|_{S_9} = -p_2,$$

$$\sigma_{12}\Big|_{S_i} = 0 \quad (i = 1, 2, \ldots, 9, 16, 17), \qquad \sigma_{21}\Big|_{S_i} = 0 \quad (i = 10, \ldots, 15, 19), \tag{6}$$

$$\sigma_{22}\Big|_{S_{13}} = -p_3, \qquad v_1\Big|_{S_1} = 0, \qquad v_2\Big|_{S_i} = 0 \quad (i = 10, 15, 19).$$

The adhesion of the ice mass (region I in Fig. 2) to the base (surface S_{19}) is described by the friction law

$$\sigma_{21}\Big|_{S_{19}} = -\psi \tau_s v_{sl}/|v_u|,$$

where $v_{sl} = v_1|_{S_{19}} - v_1^*$ is the velocity of sliding of region I (ice) relative to the base, $v_1^* = 0$ is the velocity of the base, $|v_u|$ is the normalizing velocity, and τ_s is the conditional yield point of ice; the friction coefficient ψ was set equal to 1000.

The system of equations for region IV differs from system of equations for regions I–III [except for Eqs. (3) and (5)]. For the regions $t = \text{I}, \ldots, \text{IV}$, the system of equations is written as

$$\sigma_{ij,j} + F_i^t + k_t \mu \nabla^2 v_i = I_i^t, \qquad I_i^t = \rho_t \frac{dv_i}{dt}, \qquad k_t = \begin{cases} 0, & t = \text{I}, \text{II}, \text{III}, \\ 1, & t = \text{IV}; \end{cases} \tag{7}$$

$$\sigma_{ij} - \sigma \delta_{ij} = 2 G_t \varepsilon_{ij}, \qquad G_t = 0 \quad \text{at} \quad t = \text{IV}, \qquad \varepsilon_{ij} = \int_\tau \xi_{ij} \, d\tau,$$
$$\tag{8}$$
$$\xi_{ij} = 0.5(v_{i,j} + v_{j,i}), \qquad v_{i,i} = 0.$$

In (7), $F_1^t = \gamma_1^t$, $F_2^t = 0$, $F_3^t = 0$, and γ_1^t is the relative weight of the material of the medium in the region t.

Thus, for $k_t = 0$, system (7), (8) coincides with system (1)–(3), and for $k_t = 1$, $G_t = 0$, and $t = \text{IV}$, it coincides with system (4), (5). Indeed, if $G_t = 0$, then, $\sigma_{ij} = 0$ ($i \neq j$) and $\sigma_{11} = \sigma_{22} = \sigma_{33} = \sigma$. Since $\sigma = -p$, Eqs. (7) coincide with Eq. (4).

To solve the system of differential equations (7) and (8) subject to boundary conditions (6), we use a numerical method [2, 3], in which the deformation region is divided into straight parallelepipeds of finite size; for each element, system (7), (8) is written in difference form and solved using the proposed algorithm taking into boundary conditions (6). As a result, we obtain the stress field σ_{ij} and the displacement velocity field v_i on the sides of each element.

The Laplace operator for an arbitrary element in orthogonal coordinates was obtained in the derivation of the heat-conduction equation in [2, 3].

In Eq. (7), the inertial term can be written in difference form taking into account axial symmetry:

$$I_i^t = \rho_t \left(\frac{(v_i)_m - (v_i)_{m-1}}{\Delta \tau_m} + \bar{v}_1 \frac{(\Delta v_i)_1}{\Delta x_1} + \bar{v}_2 \frac{(\Delta v_i)_2}{\Delta x_2} \right). \tag{9}$$

Here $(\Delta v_i)_k$ ($k = 1, 2$) is the change in the velocity v_i along the coordinate α_k, $\bar{v}_i$ are the average velocities v_i over an element which are frozen in the nth iteration [$(\bar{v}_i)_n = (v_i)_{n-1}$], and $(v_i)_m$ and $(v_i)_{m-1}$ are the average velocities of motion over an element in the time steps $\Delta \tau_m$ and $\Delta \tau_{m-1}$.

Algorithm of Solution of the Problem. The algorithm for the solution of the problem is constructed using the technique described in [4, 5].

1. The entire deformation process is divided into m steps in time τ.

2. The initial conditions at $\tau = 0$, the matrix G_t ($t = \text{I}, \ldots, \text{IV}$), and the quantities $v_i|_{m=0} = 0$ and $\varepsilon_{ij}|_{m=0}$ are specified.

3. The time step $\tau = \Delta \tau$ is specified.

96

4. The examined deformation region is divided into orthogonal elements. The matrix of the lengths of arcs of the elements is calculated. Identification of the region for the parameter k_t ($t = \mathrm{I}, \ldots, \mathrm{IV}$) is performed.

5. Boundary conditions are specified.

6. In formula (9), the values of $(v_i)_m$ and $\bar{v}_i$ for each element are specified. In this case, system (7), (8) written in difference form according to [2, 3] is linear.

7. The matrix of coefficients and free terms of the new equivalent system is calculated using the technique described in [5].

8. The system of linear equations is solved by a standard program.

9. The quantities σ_{ij}, v_i, and $(\varepsilon_{ij})_m$ are calculated for each element and its sides.

10. The values of $(\bar{v}_i)_n = (\bar{v}_i)_{n-1}$ are specified.

11. The quantities $(\bar{v}_i)_n$ and $(\bar{v}_i)_{n-1}$ (n is the iteration number) are compared with each other. If the specified accuracy of correspondence between $(\bar{v}_i)_n$ and $(\bar{v}_i)_{n-1}$ is reached, operation 12 is performed; otherwise operation 7 is performed.

12. The new parameters of the gap H_4 due to the divergence of the cylinders are calculated. The orthogonal grid is corrected. The following assignments are made: $(\varepsilon_{ij})_m = (\varepsilon_{ij})_{m-1}$ and $(v_i)_m = (v_i)_{m-1}$.

13. The new pressure parameters in region V are calculated using the adopted law $pV = \mathrm{const}$ (isothermal process), where p and V are the gas pressure and volume in region IV, respectively.

14. Calculations are performed in the time step $\Delta\tau_m$.

15. If $\tau < \sum_m \Delta\tau_m$, operation 5 is performed; otherwise, operation 16 is performed.

16. End of the calculation.

Results of Solution of the Problem. For natural gas (containing 9.9% methane), the burning velocity is $v_\mathrm{b} \simeq 0.67$ m/sec, with the pressure in the closed volume reaching 6–7 atm [1].

We assume that during the burning time $\tau_\mathrm{b} = H_4/v_\mathrm{b}$, the pressure between the cylinders increases linearly. In this case, the cylinders diverge, and, hence, the pressure between them decreases.

The following initial geometrical parameters are adopted (see Fig. 2): $H_1 = 2$ m, $H_2 = 0.1$ m, $H_3 = 1$ m, $H_4 = 0.03$ m, $H_5 = 0.1$ m, $H_6 = 1$ m, $R_1 = 3$ m, $R_2 = 3.1$ m, $R_3 = 3.2$ m, $R_4 = 4.2$ m, and $R_5 = 30$ m. In this case, $p_1 = 1$ atm and $p_2 = 1.5$ m. The problem was solved in time steps $\Delta\tau_m$ ($\tau = \sum_m \Delta\tau_m$). The pressure was set equal to 4.74 atm. The burning time was $\tau_\mathrm{b} = 0.045$ sec.

According to reference data [6, 7], the following values of the elastic moduli for ice and steel were adopted: $G_1 = 29.2 \cdot 10^3$ kg/cm^2 and $G_3 = G_4 = 8 \cdot 10^5$ kg/cm^2. The viscosity of water was equal $\mu = 0.01789$ g/(cm$^2 \cdot$ sec) at a temperature equal to 0°C. The relative weights were set equal to $\gamma_1 = 920$ kg/m^3, $\gamma_2 = 1000$ kg/m^3, and $\gamma_3 = \gamma_4 = 7800$ kg/m^3.

According to [6], we assume that, in the case of tension, ice breaking occurs at $\sigma_\mathrm{b} = 1.5$ MPa, and in the case of compression, it occurs at $\sigma_\mathrm{c} = 2.5$ MPa. The calculation results show that in a radius approximately equal to 5 m, the ice cover is completely broken and is ejected upward at a velocity of 1.35 m/sec; ice breaking occurs in both tangential and in radial directions.

Significant elastic deformations also occur in the metal structure, with the tensile stress reaching 125 MPa. The yield point of soft St. 3 steel is $\tau_s = 30$ kg/mm$^2 = 300$ MPa, i.e., the stresses in the structure are significant but do not reach the critical value. Figure 2 shows the points at which the stresses reach the maximum value: the points A and B at the center of the lower cylinder ($\sigma_{22} = -88$ and 102 MPa, respectively), the points C and D in the transition area of the lower cylinder ($\sigma_{11} = 125$ and -118 MPa, respectively), and the points E and F on the upper cylinder ($\sigma_{11} = 102$ and -75 MPa, respectively).

The stresses in water (region IV) are equal to the hydrostatic stress: $\sigma_{11} = \sigma_{22} = \sigma_{33} = \sigma$. In this case, if the water pressure inside the cylinders is 4.75 atm, then behind the cylinders, it is 1.57 atm and remains almost unchanged with variation in p_3. In regions I, II, and III, the stresses σ_{33} reach the maximum values at the same points A and B as the stresses σ_{22}, but $|\sigma_{33}| < |\sigma_{22}|$ ($\sigma_{33} = -87$ MPa and $\sigma_{22} = 100$ MPa). At the time $\tau = \tau_\mathrm{b}$, the velocity of the upper cylinder is $v_1 = 1.35$ m/sec, the velocity of the lower cylinder $v_1 = -9.8$ m/sec, and the ejection velocity of ice is $v_1 = 1.35$ m/sec. In the zone which is peripheral for the cylinders, the velocity and direction of motion of water correspond to the kinematics of movement of the cylinders.

Conclusions. The results of the numerical calculations show that the proposed method leads to complete breaking of ice cover (jam). Ice is broken into small chips under the stresses produced and is ejected upward by the bottom of the upper cylinder.

The structure of the metal cylinders is subjected to significant stresses which do not exceed the elastic limit.

By the action of the pressure p_3, the lower cylinder is pushed downward at a velocity greater than the velocity of lift of the upper cylinder. This should be taken into account because the displacement velocities are considerable, which can lead to a failure of the restriction system which prevents the lower cylinder from falling out of the upper cylinder. In addition, as the lower cylinder moves downward and the upper cylinder upward, the volume of the gas chamber V increases sharply (see Fig. 1), resulting in a decrease in the pressure p_3.

REFERENCES

1. M. B. Ravich, *Flameless Surface Combustion* [in Russian], Izd. Akad. Nauk SSSR, Moscow–Leningrad (1949).
2. V. I. Odinokov, *Numerical Study of the Deformation of Materials Using a Coordinate-Free Method* [in Russian], Dal'nauka, Vladivostok (1995).
3. V. I. Odinokov, B. G. Kaplunov, A. V. Peskov, and A. A. Bakov, *Mathematical Modeling of Complex Technological Processes* [in Russian], Nauka, Moscow (2008).
4. V. I. Odinokov and A. M. Sergeeva, "Mathematical modeling for one new method of breaking an ice cover," *J. Appl. Mech. Tech. Phys.*, **47**, No. 2. 266–273 (2006).
5. V. I. Odinokov, A. M. Sergeeva, and E. A. Zakharova, "Mathematical model for ice cover breaking," *Mat. Model.*, **20**, No. 12, 15–26 (2008).
6. V. V. Bogorodskii and V. P. Gavrilo, *Physical Properties. Modern Methods of Glaciology* [in Russian], Gidrometeoizdat, Moscow (1980).
7. V. A. Krokha, *Hardening of Metals by Cold Plastic Deformation: Handbook* [in Russian], Mashinostroenie, Moscow (1980).